Nuclear Instruments and Methods in Physics Research A 386 (1997) 235–248

ELSEVIER

NUCLEAR INSTRUMENTS & METHODS IN PHYSICS RESEARCH Section A

A cylindrical drift chamber with azimuthal and axial position readout

Z. Bar-Yam[a,*], J.P. Cummings[a], J.P. Dowd[a], P. Eugenio[a], M. Hayek[1,a], W. Kern[a], E. King[a], N. Shenhav[a], S.U. Chung[b], R.W. Hackenburg[b], C. Olchanski[b], D.P. Weygand[b], H.J. Willutzki[b], B.B. Brabson[c], R.R. Crittenden[c], A.R. Dzierba[c], J. Gunter[c], R. Lindenbusch[c], D.R Rust[c], E. Scott[c], P.T. Smith[c], T. Sulanke[c], S. Teige[c], S. Denisov[d], A. Dushkin[d], V. Kochetkov[d], V. Lipaev[d], A. Popov[d], I. Shein[d], A. Soldatov[d], E.V. Anoshina[e], V.A. Bodyagin[e], A.I. Demianov[e], A.M. Gribushin[e], O.L. Kodolova[e], V.L. Korotkikh[e], M.A. Kostin[e], A.I. Ostrovidov[e], L.I. Sarycheva[e], N.B. Sinev[e], I.N. Vardanyan[e], A.A. Yershov[e], T. Adams[f], J.M. Bishop[f], N.M. Cason[f], A.H. Sanjari[f], J.M. LoSecco[f], J.J. Manak[f], W.D. Shephard[f], D.L. Stienike[f], S.A. Taegar[f], D.R. Thompson[f], D.S. Brown[g], T. Pedlar[g], K.K. Seth[g], J. Wise[g], D. Zhao[g], G.S. Adams[h], J. Napolitano[h], M. Nozar[h], J.A. Smith[h], M. Witkowski[h]

[a] *University of Massachusetts Dartmouth, North Dartmouth, MA 02747, USA*
[b] *Brookhaven National Laboratory, Upton, L.I., NY 11973, USA*
[c] *Indiana University, Bloomington, IN 47405, USA*
[d] *Institute for High Energy Physics, Protvino, Russian Federation*
[e] *Institute of Nuclear Physics, Moscow State University, Moscow, Russian Federation*
[f] *University of Notre Dame, Notre Dame, IN 46556, USA*
[g] *Northwestern University, Evanston, IL 60208, USA*
[h] *Rensselaer Polytechnic Institute, Troy, NY 12180, USA*

Received 5 August 1996

Abstract

A cylindrical multiwire drift chamber with axial charge-division has been constructed and used in experiment E852 at Brookhaven National Laboratory. It serves as a trigger element and as a tracking device for recoil protons in π p interactions. We describe the chamber's design considerations, details of its construction, electronics, and performance characteristics.

Keywords: Partial detector; Drift chamber; Cylindrical charge division

1. Introduction

We report here on the construction and operation of a cylindrical drift chamber (TCYL) of a new design. The chamber measures azimuthal and axial positions of charged particle trajectories. Some of the chamber's components, in particular its cylindrical cathodes, have been built using techniques we have developed previously [1]. However, event topologies, the need for axial (z) position measurement, and severe geometric constraints resulted in an overall unique design.

Experiment E852 at Brookhaven National Laboratory (BNL) is designed to study both neutral and charged final states of π^- p collisions in a search for gluonia, hybrid, and multi-quark mesons. An 18 GeV/c π^- beam from the alternating gradient synchrotron (AGS) is incident on a liquid hydrogen target located in the large 1.0 T magnet of BNL's multi-particle spectrometer (MPS). The spectrometer instrumentation includes detectors for identifying and tracking the incoming beam particles and their interaction

* Corresponding author. Tel. +1 617 738 5135, fax +1 617 738 8722, e-mail zbaryam@umassd.edu.

[1] Permanent address: Rafael, Haifa, Israel.

PII S0168-9002(96)01032-7

products. The detection system includes 47 planes of proportional and drift chambers measuring charged particle trajectories in the MPS magnetic field, augmented by neutral particle detectors that include a 3045-element lead glass calorimeter (LGD) [2], a lead-scintillator sandwich detector (DEA), and a 198-channel cesium iodide barrel (CIB) and end ring (CIR) detector [3]. See Fig. 1 for the general experimental setup and Fig. 2 for the target region.

The MPS facility's trigger electronics and data acquisition system have been upgraded for E852, permitting data taking rates of up to 700 events per AGS beam spill (2×10^6 particles) with less than 60% dead time. Several triggers operating simultaneously select events with all-neutral final states, states of various charge multiplicity that also contain at least one photon pair, and charged states without any photon requirements. The trigger design permits the concurrent acquisition of data on many distinct reactions.

As a trigger element, TCYL detects single large-angle recoil proton tracks emerging from the target and vetoes events with more than one large-angle track. It also identifies the absence of such tracks for processes involving a recoil neutron. As an off-line tracking device, TCYL measures the recoil proton trajectory which in this experiment has lab angles of typically 50 to 60° and momenta between 0.1 and 1.7 GeV/c. In the off-line analysis, TCYL is used in the overall event reconstruction including the localization of the production vertex. In addition, it is used for tracking charged particles to the CIB detector so that the energy deposited by them in the CIB can be subtracted when the CIB is used to reject events with large-angle photons.

TCYL's role in vertexing is crucial for event topologies with only a single charged track in the forward direction such as the reaction $\pi^- p \to \eta\pi^- p$ (with $\eta \to \gamma\gamma$). This channel is important in a search for exotics decaying to $\eta\pi^-$, and TCYL is needed to measure the recoil proton track and accurately establish the production vertex. In other channels of E852, TCYL has been of great value at the trigger level for identifying events with exactly zero, one, or more than one recoil track. TCYL is able to reconstruct multiple tracks traversing it in a single event.

TCYL surrounds the target inside the CIB. Its radial dimensions are constrained by the o.d. of the target jacket and by the i.d. of the CIB (see Fig. 2). Limiting the CIB's inner radial dimension was driven by cost considerations.

The TCYL chamber was constructed and tested during 1992–93 and met all design specifications. It has operated exceptionally well during extensive runs in 1993, 1994, and 1995.

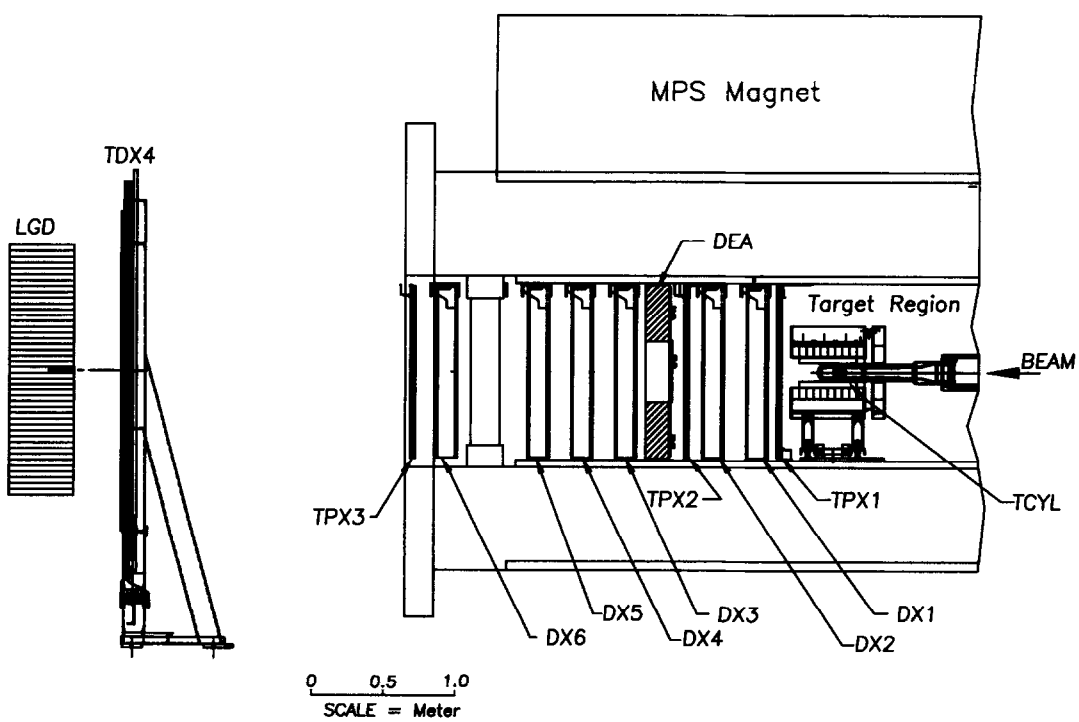

Fig. 1. Diagram of the E852 spectrometer (side view). Located inside the 1.0 T magnetic field of the multi-particle spectrometer (MPS) are: the cylindrical drift chamber (TCYL) and cesium iodide detector surrounding the target; three tracking proportional chambers (TPX1–TPX3); six drift chambers (DX1–DX6); and the lead-scintillator downstream endcap array (DEA). Downstream of the MPS magnet are a large drift chamber (TDX4) and the 3045-element lead glass detector (LGD).

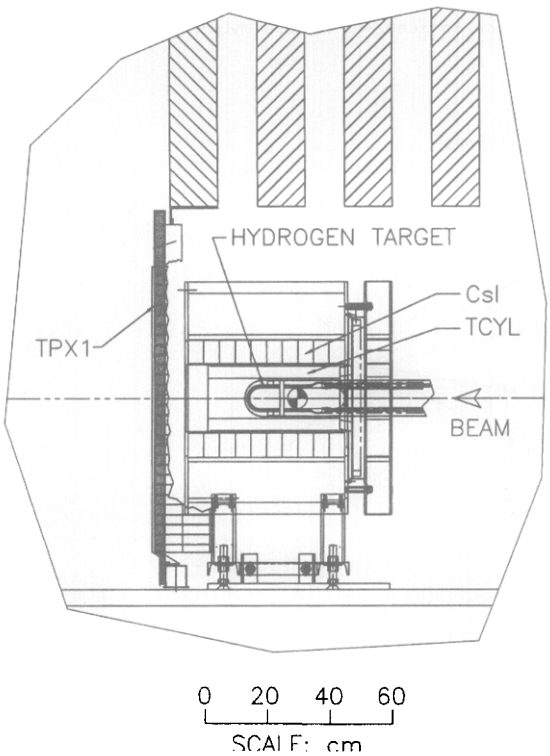

Fig. 2. Side view of the E852 target region. The hydrogen target is surrounded first by the cylindrical drift chamber (TCYL) and then by the cesium iodide veto detector (CsI).

2. Design considerations

The requirements of the physics to be studied and the geometric constraints imposed by the experimental setup led us to adopt the following design criteria:

(i) To ensure good particle-track definition, the chamber had to have at least four layers of sense wires. Isolation of the layers was achieved by using solid cathodes between them so that one malfunctioning layer would not bring down the whole chamber.

(ii) To permit the use of the chamber as a trigger device at a high data acquisition rate, the maximum drift time and thus the cell size had to be small. The cell size was chosen so that the maximum drift distance was about 4 mm corresponding to 80 ns drift time.

(iii) To measure proton tracks recoiling from interactions in the H_2 target, the chamber had to be the innermost detector, surrounding the target with minimum material. It also had to have limited radial dimension since it was to be nested inside the CsI detector (CIB), the cost of which would increase drastically with radial size. The cylindrical space allocated for the chamber was between the outside jacket of the target (114 mm o.d.) and the inside wall of the CsI barrel detector (210 mm i.d.). This limited the chamber to a total radial thickness of 37 mm with 5–6 mm clearance on both sides.

(iv) To reduce interactions and multiple scattering of the particles traversing it, the chamber had to be constructed using materials of low-Z and minimum mass. Our past experience using laminates of Rohacell® and Kevlar®[2] was of much help in that respect. In addition, the small size of the chamber, the use of shared cathodes between neighboring sense layers, and low wire tension permitted a reduction in structural material.

(v) To detect recoil protons from the downstream end of the target required the chamber's sensitive volume to extend beyond that point. Since the target length was set to be 30 cm, the sensitive length of the chamber was chosen to be 40 cm to accommodate typical recoil proton production angles throughout the hydrogen target volume.

(vi) To employ the charge division technique for measuring the location of ionization along the axial direction required use of a resistive wire. The eventual choice for the sense wire was 21.85 Ω/cm, 0.8 mil thick wire made of stainless steel alloy.

(vii) To prevent excessive material in the path of particles no electronic components could be placed at the downstream end of the chamber. This posed a major challenge since the charge division method requires collection of the charge from both ends of the wire. We solved this problem by connecting the sense wires in pairs at the downstream end, and reading them out using electronics mounted on the upstream end.

(viii) To cope with the electronically noisy MPS environment, it was necessary to amplify the primary ionization signals before sending them via coaxial cable to the trigger and to the data acquisition electronics. This requirement resulted in the choice of thin (0.8 mil) sense wire and use of preamplifiers mounted directly on the chamber.

3. Chamber description

TCYL is a drift chamber with four layers of sense (anode) wires strung axially along cylindrical surfaces surrounding the liquid H_2 target (see Fig. 3). The four layers have 54, 60, 68, and 74 sense wires alternating with an equal number of field wires in each layer. The wires are located at a radial distance of 68, 77, 86, and 95 mm, respectively, from the cylinder axis. The sensitive wire length is 40 cm. Solid aluminized cylindrical cathodes located midway between the wire layers establish the drift gaps. The chamber extends radially from 63 to 100 mm.

The chamber is constructed of five nested concentric cylinders forming between them four annular gaps. The cylinders are aluminized on their surfaces facing the gaps and provide cathodes and gas confinement for each of the gaps. At their ends the cylinders are fitted with rings that

[2] The supplier of Kevlar cloth was Hi-Pro-Form-Fabrics Inc., 962 Devon Drive, Newark, DE 19711, USA.

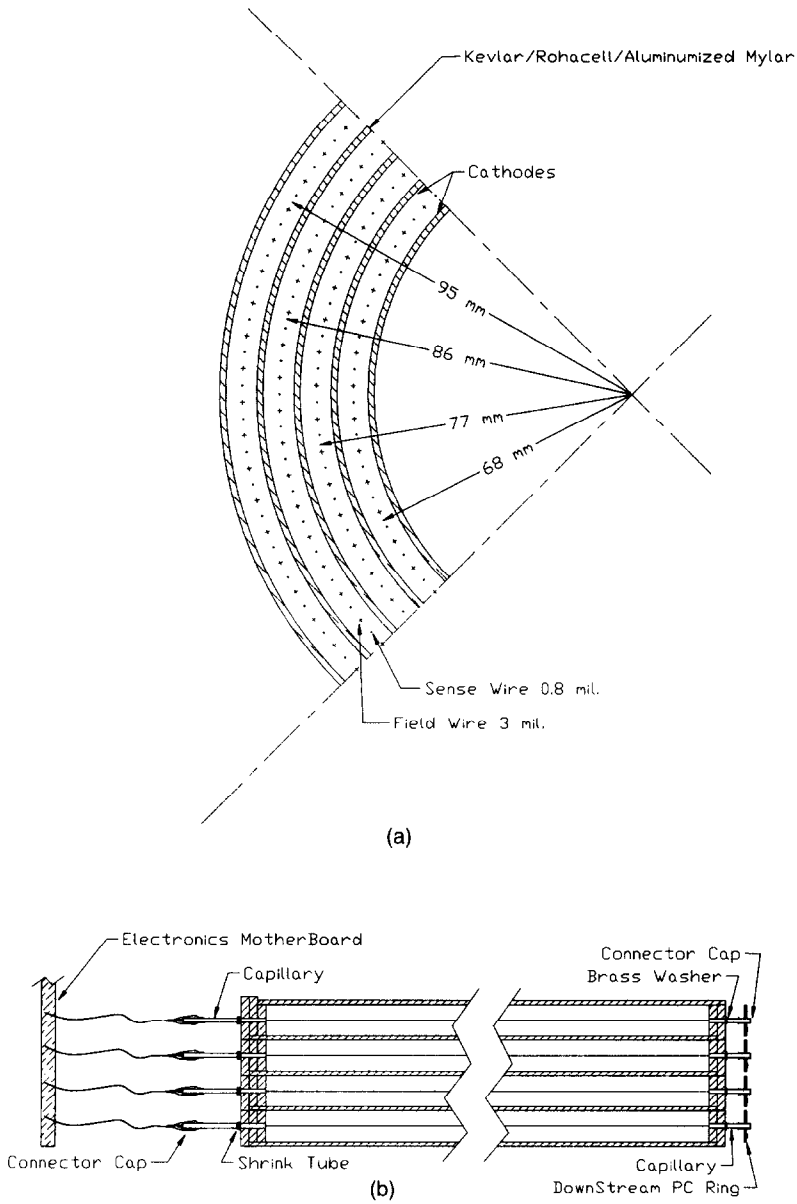

Fig. 3. (a) Partial cross-sectional view of TCYL. (b) Longitudinal cross-sectional view of TCYL.

complete the gas enclosure of each gap. These rings support the sense and field wires strung through molded holes midway between the cathodes. The radial distance from the sense wires to each of the cathode cylinders is 4.0 mm and the sense and field wires alternate every 4 mm, forming a drift cell of 80 ns maximum drift time. The rings at the ends of the cylinders fit one inside the other to form an annular disc that gives the chamber its structural integrity and provides a support for the readout electronics.

The structural components of the chamber, i.e. the cylindrical walls and the end rings, were made using refinements of the general lamination method described in Ref. [1]. These refinements were needed due to the stringent space constraints. Here the walls are only 1 mm thick and the adjacent gaps share the walls that separate them. The two exterior cylindrical walls of the chamber, i.e. the smallest and the largest cylinder, consist of single layers of Kevlar, Rohacell, and aluminized Mylar. The three interior walls shared by the gaps are built similarly but have layers of aluminized Mylar on their inside and outside surfaces to provide cathodes to both of the adjacent gaps. The aluminized Mylar consists of 2 mil Mylar laminated with 1 mil aluminum. The Kevlar is a woven cloth 4 mil thick, and the Rohacell, originally 2 mm thick stock, was machined to give a total wall thickness of 1 mm. The cylinders were formed, laminated with epoxy,

and machined on aluminum mandrels of precise dimensions. The area density of a cylindrical wall is 0.06 g/cm^2.

The end rings were made of the same materials as the cylinders but were laminated on specially instrumented jigs and then were machined to the required diameters. The downstream rings have two layers of Rohacell sandwiched between layers of Kevlar. Their total density is 0.11 g/cm^2. The density of the upstream rings was not so critical and since these rings support the electronics they were made sturdier using three layers of Rohacell laminated between four layers of Kevlar.

During the lamination of the rings, 5 mil diameter holes were molded approximately every 4 mm along the middle circumference of the rings. These holes house alloy capillaries[3] that are crimped onto the wires to secure them and maintain their tension. The 0.8 mil diameter stainless steel sense wires are at 19 g tension and the 3 mil diameter stainless steel field wires are at 150 g. After reviewing the dimensional stability of the support structure for the wires, we found it unnecessary to spring-load the wires as in our previous design and we did not experience failures due to wire-breaking. Our method for measuring wire tension was described earlier [4].

Before stringing the wires, holes were drilled in the end rings for gas tubes and for the cathode high voltage supply wires. The gas mixture (80% argon, 15% isobutane, and 5% methylal) was supplied by the central MPS gas system. The chamber gas inlet is located at the bottom of the downstream end and the exhaust at the top of the upstream end of each gap for optimal filling and flushing of the chamber and for avoiding air pocket formation. Additional ports are provided for monitoring the gas pressure in each gap.

The wire-stringing was carried out for each gap separately. Then each module, composed of the individual inner cylinder with end rings attached and wires strung on the outside, was inserted into the adjacent module, and thus, the whole chamber was successively nested from inside out. Insertion into the outermost cylinder completed the assembly. To prevent wire breaking during the nesting process a special tool was constructed to guide the modules while they were lowered one onto the other (see Fig. 4).

The end rings were sealed to each other using 5 min epoxy and super bond. Before applying epoxy, a thread was inserted into the groove between rings to allow easy removal of the seal if this should be needed for disassembly. After gluing, the rings form a sturdy annular disc at each end of the chamber.

For mechanical support of the chamber, G-10 rims were fitted onto the outer edge of both end discs. The rims have an L-shaped profile and extend 4.0 mm beyond the radial dimension of the chamber so that the chamber can rest on

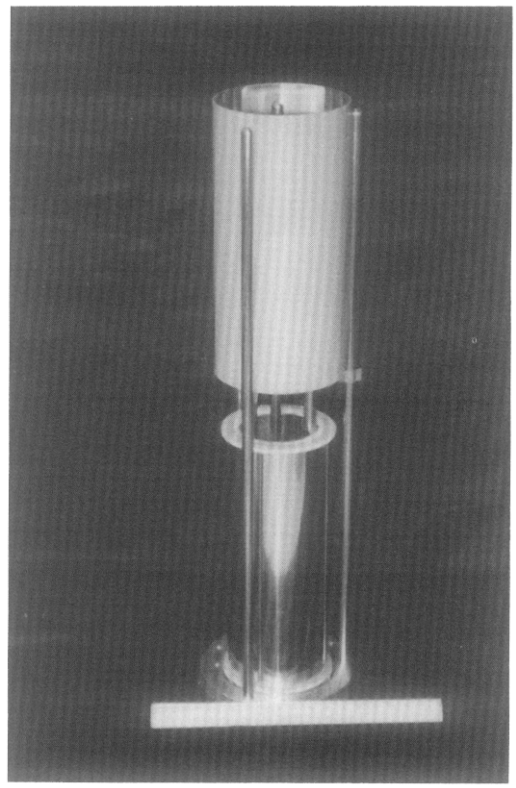

Fig. 4. The nesting tool, consisting of movable rods mounted on a base plate. The rods constrain and guide the cylinders during their nesting.

them rather than on the delicate cylinder. Holes drilled in these rings provide passage for gas input tubes and calibration signal cables that run along the outside surface of the outer cylinder. The gas tubes are 60 mil o.d. polyethylene tubes. The calibration signals are delivered through eight RG-174 coax cables to the injection capacitors on the downstream printed circuit (PC) rings.

Fig. 5 shows the chamber after it was sealed, fitted with the supporting G-10 rims and with gas tubes installed. At that stage of assembly the capillary tubes that hold the sense and field wires were trimmed on the outside of the downstream rings. The field wire capillaries were cut at the wire-retaining crimp while the sense wire capillaries were left 2 mm longer to accept small end-cap socket connectors[4]. Thin PC rings with precision holes for all capillaries were aligned over these connectors and then carefully pushed onto them. The end-cap sockets on the sense wire capillaries fit snugly through the holes and were soldered to pads on the PC ring. The shorter field wire capillaries fit into clearance holes in the PC rings without making electric contact. The downstream PC rings provide

[3] Superior Tube Co., P.O. Drawer 191, Norristown, PA, USA.

[4] AMP Special Industries, 25 Commerce Drive, Cranford, NJ 07016, USA.

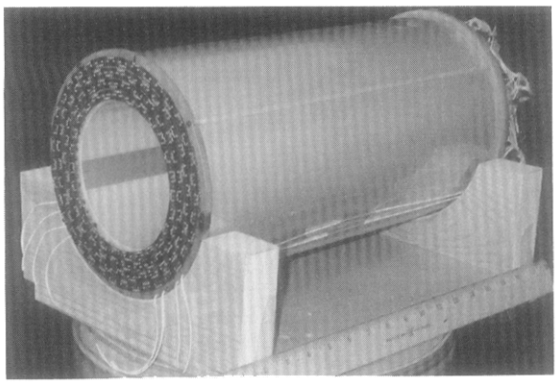

Fig. 5. The completely nested TCYL before attachment of the upstream motherboard. The downstream PC rings and their RC network are visible at the left. The chamber rests on its G-10 flanged rims at both ends.

a calibration-signal distribution network and a resistive–capacitive (RC) connection to pair consecutive sense wires. See description of the electronics below.

On the upstream end, a large PC motherboard is mounted directly on the end disc via flexible standoffs 2.5 in. long. The capillaries on this side of the sense wires are connected to a preamplifier stage of the readout electronics located on the board. The standoffs are unable to support all the weight of the motherboard and serve mainly to set its position relative to the chamber. When the chamber is operating inside the CIB, the main mechanical support for the motherboard is provided by attaching it to the hexagonal face of the CIB box. During assembly and testing, the chamber and the motherboard were supported by a mockup of the CIB box made of lucite. To transfer the chamber from the mockup to the experiment site we used a lucite pipe that snugly fit inside the TCYL cylinder and protruded through the upstream end so that it supported the motherboard during transport.

In addition to the first stage of the readout electronics, the motherboard carries HV distribution pads for the cathodes and field wires and manifolds for gas distribution.

4. Chamber electronics

The charge division method for measuring track positions of particles traversing a chamber usually requires readout of the sense wires at both ends [5]. However, we adopted a different scheme. We designed each of the four gaps with an even number of resistive sense wires and connected adjacent sense wires into pairs via a simple RC network at TCYL's downstream end. A sense wire pair could thus be treated as a single wire and be read out at the upstream end. This allowed placement of all the readout electronics at TCYL's upstream end, thus minimizing the material downstream without sacrificing spatial resolution along the axial direction.

A block diagram of the electronics is shown in Fig. 6. At the upstream end, the sense wires are connected by short wires to 256 preamplifiers on the motherboard, one for each sense wire. The motherboard also contains the distribution wiring of the negative high voltage to all cathode and field wires and of the calibration signal to all sense wires. The 256 preamplifier outputs are sent via 100-ft coaxial cables to the inputs of shaping amplifier modules. These modules produce two different kinds of output signals.

The first is an analog pulse generated by slow shaping-amplifiers for pulse height analysis via ADCs, and the second is a fast timing signal generated by fast amplifiers followed by discriminators that produce an ECL pulse for TDCs. The 256 ADCs measure the amount of charge arriving at both upstream ends of every sense wire pair and thus provide both the identification of the wire that fired in the pair and the axial position of the track passing through TCYL. The TDCs measure the ionization drift time and thus provide the azimuthal distance of the track from the wire that fired. The left to right ambiguity of the ionization distance from a sense wire is removed by using the information from the four layers of staggered sense wires. Since there is only one fast amplifier per pair of sense wires (128 in total), the identification of the wire in the pair which fired is obtained from the ADC signal.

In order to be used in the event trigger, the 128 discriminator output signals are also sent to four-fold fan-ins for channel reduction. The 32 outputs from these circuits are used in multiplicity logic units. This scheme allowed us to select events with a definite number of hits in each layer of TCYL; see Section 4.3 below.

4.1. Readout circuit

A schematic of the preamplifier stage of the readout circuit for one sense wire pair is shown in Fig. 7. The RC network connecting sense wires in pairs consists of two 50 Ω resistors and a 0.1 μF capacitor surface-mounted on a thin (25 mil) PC downstream ring. The two resistors prevent ambiguous wire identification (in the pair) when the hit location is close to the connected wire ends downstream. The capacitor provides dc isolation between the two preamplifiers located upstream on the motherboard. The additional 50 Ω resistors connected in series in front of the preamplifiers reduce the dynamic range of the charge signal. Calibration signals are fed to the middle and also to the ends of the wire pair through three 2 pF capacitors.

The downstream rings are four-layer PC boards. The uppermost layer carries the components that interconnect the sense wires. The 2 pF calibration capacitors are realized by micro strips. The second layer includes the calibration signal distribution line and the attached

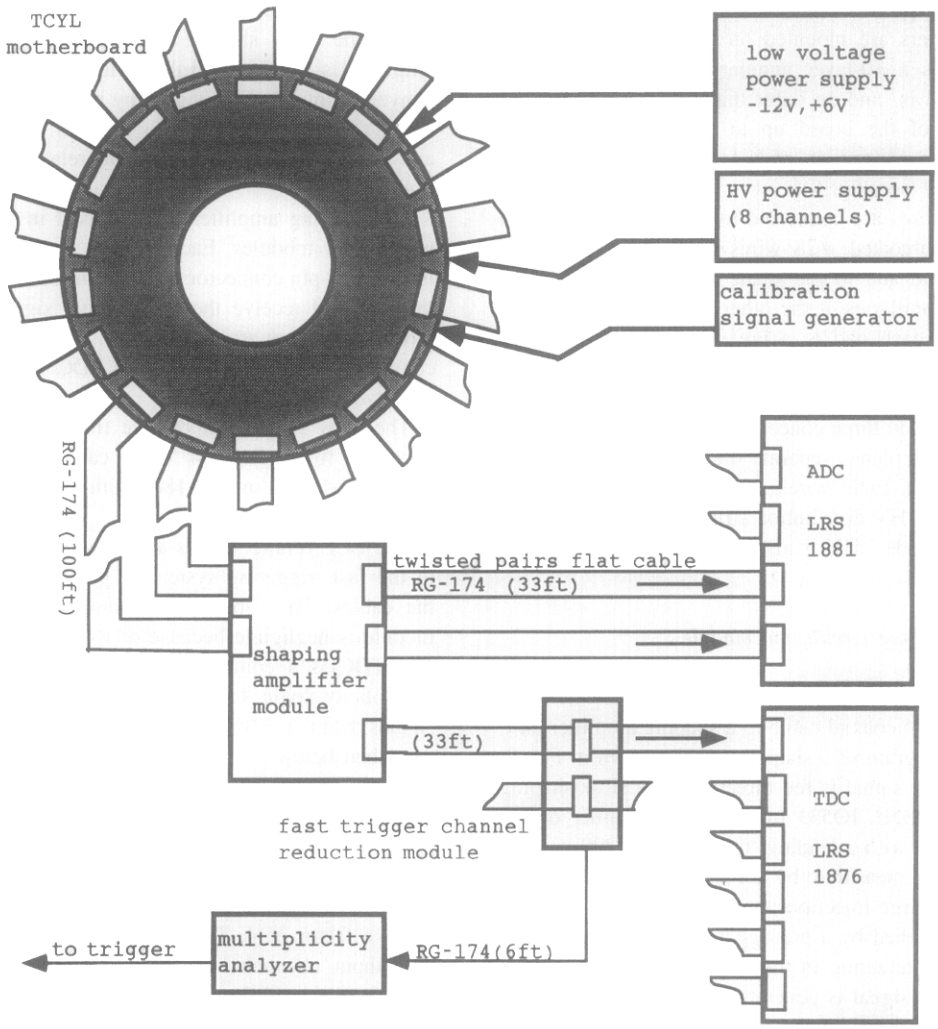

Fig. 6. Block diagram of the TCYL detector electronics.

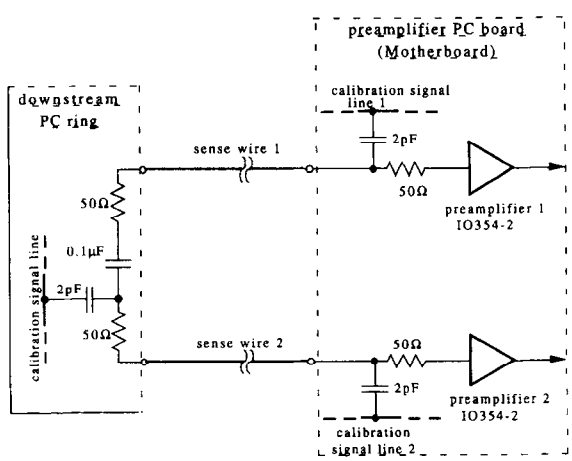

Fig. 7. A schematic diagram of the preamplifier stage of the TCYL readout circuit for one sense wire pair.

capacitor pads, the third layer has the capacitor pads that are connected to the link network and the fourth layer is a ground plane.

The preamplifier is a modified version of the BNL type IO354-2 [6], common base input, hybrid with a gain reduced by a factor of 5. This gain adjustment was needed to minimize saturation of amplifiers and ADCs while maintaining the cathode voltage high enough to raise the signal well above the pickup noise. By optimizing the preamplifier gain we could operate at -1.7 kV for both cathode and field wire potential. This has given us sufficient primary gain in the chamber to yield a good margin of safety against both amplifier overload and HV-induced gas discharge problems since the streamer mode was found to occur above 2 kV.

The resistance of each sense wire is about 875 Ω and the total resistance of a wire pair with the series resistors between them is 1.850 kΩ. There are 128 pairs of sense

wires requiring preamplifiers on both ends, thus a total of 256 preamplifiers are mounted on the motherboard. The motherboard is a 10-layer annular board with an inner diameter of 10 in. and an outer diameter of 21.5 in. The inner section of the board up to a diameter of 13 in. contains all the connection pads for the chamber's sense and field wires (see Fig. 8).

The sense wires are connected to the input pads by 2.5 in. long Teflon-coated #28 wires soldered to the board pads at one end and to the small cap connectors on the sense wires' capillaries at the other end. A printed circuit strip connects each pad to a preamplifier. The two preamplifiers of a sense wire pair are treated as a distinct unit cell on the motherboard. The 128 preamplifier cells are laid out on the board in three concentric circles. Ground planes and bias voltage planes separate the signal strip layers to prevent crosstalk. Field wires are grouped in triplets and are connected to HV distribution strip rings on the motherboard. The cathodes' HV is also supplied through pads on the board.

4.2. Signal shaping circuit and module

The output of each preamplifier unit is transmitted via 100 ft of RG-174 coaxial cable to a shaping amplifier unit. A schematic diagram of a shaping unit is shown in Fig. 9. The preamplifier signal is fed directly into a slow shaping amplifier, type BNL IO533 hybrid. The amplifier output signal is bipolar with a leading lobe width of 200 ns. The pulse height is measured by an ADC, and is used to calculate the charge injection position along the wire. The ADC gate is opened by a pretrigger signal generated by a beam particle interacting in the target.

A fast timing signal is generated by feeding the sum of the preamplifier signals into a fast shaping amplifier, type BNL IO532-1 hybrid. This hybrid was modified by bypassing the internal resistor and capacitor connected in series with the input of the shaper, to provide a low impedance summing point for preventing crosstalk between the slow shaping amplifiers. The output of the amplifier is a unipolar pulse with a width of 12 ns. It is converted into an ECL signal by a fast discriminator, type BNL AD96685. This signal is used for triggering purposes and for measuring the drift time relative to a reference timing signal.

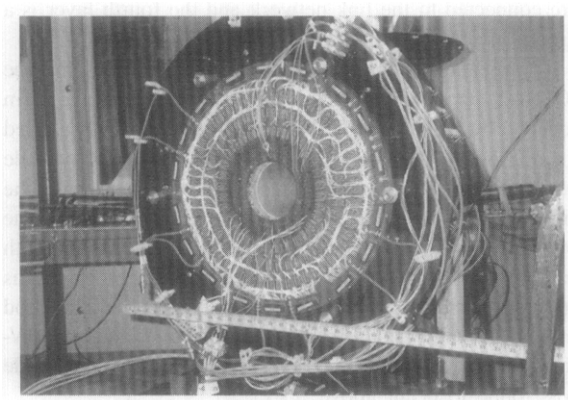

Fig. 8. TCYL mounted inside the CsI housing box. The motherboard carries all components of 256 preamplifiers and their connection pads.

The shaping amplifiers are encased in standard 3-unit-width NIM modules. Each module contains 16 units and five 2×17-pin connectors. Two of these connectors are on the rear and receive the preamplifier signals, two out of three on the front are for the ADC signals transmitted over coax cables, and one is for the TDC signals transmitted over twisted-pair flat cable.

The slow shaper outputs are transmitted to the ADCs over 33 ft of RG-174 coax cables. The ADC is a commercial LRS[5] model 1881 with inputs wired to receive signals into 50 Ω.

The ECL timing signals are transmitted to the TDC and to the fast triggering system in parallel over twisted-pair flat cables. The cable loading due to the fast triggering module is negligible because of its high input impedance. The TDC is a commercial LRS model 1876, while the multiplicity logic for the triggering system receives its signals from a BNL-designed channel reduction module described below.

4.3. Channel reduction module (CRM) and multiplicity logic

The CRM can reduce the number of input channels by up to a factor of 4. There is one "OR" output for every four input channels, altogether 16 output channels in a module. We used four such modules, one for each of the concentric cylindrical wire layers.

As a result of the pairing of wires we have 27, 30, 34, and 37 signals from the four wire layers that are fed to the four CRMs, respectively. We obtain 8, 8, 9, and 10 outputs from the CRMs each representing a subdivision of the wires in a layer. The CRM outputs are NIM signals and they are fed into multiplicity analyzer units (MAU) [7], one per layer. Each MAU unit receives pulses from a CRM representing a particular wire layer and generates two NIM signals: (1) an "OR" signal when there is at least one hit in the chamber; (2) a multiplicity signal, when a preselected number of hits has been acquired. These signals are used in the fast trigger logic of the experiment.

5. Calibration and testing

TCYL was calibrated and studied using ^{55}Fe and ^{106}Ru sources and cosmic rays prior to its insertion into the

[5] LeCroy Research Systems, Chestnut Ridge, NY, USA.

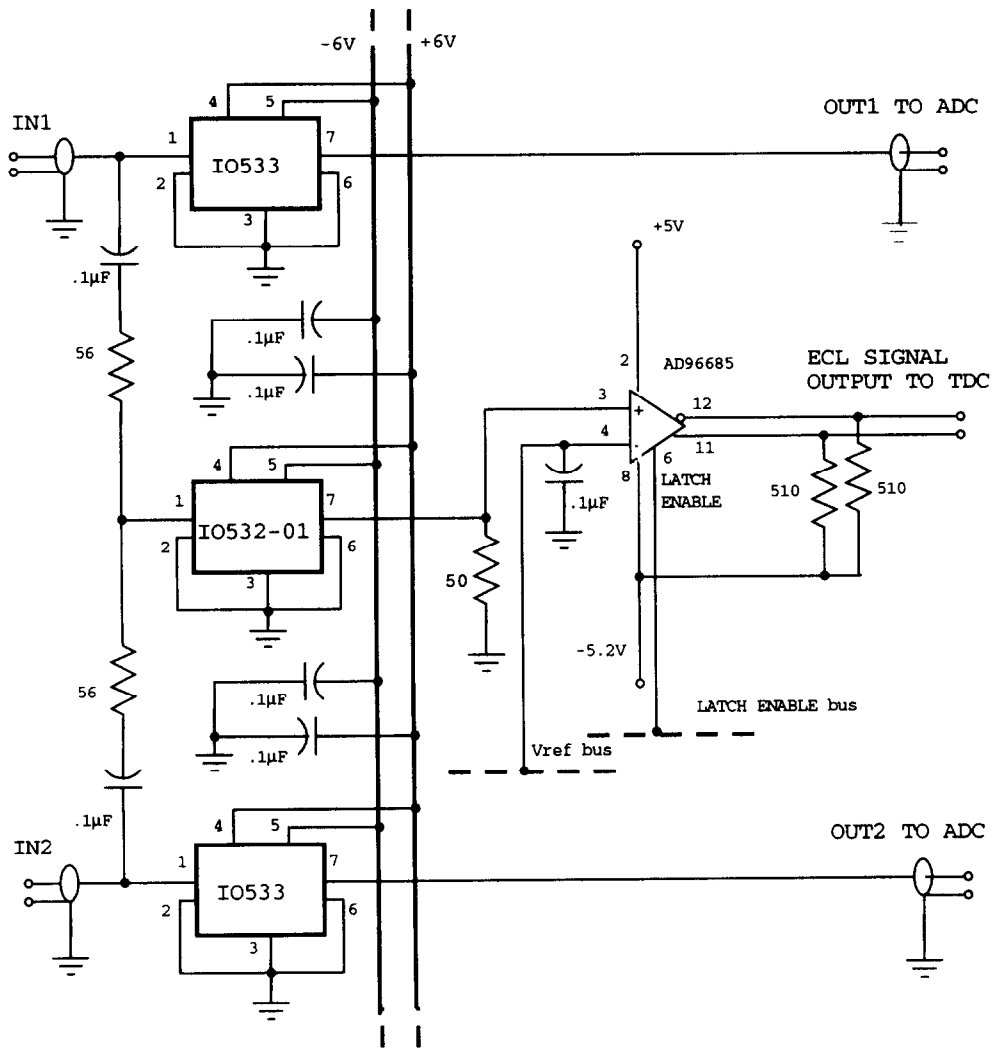

Fig. 9. Circuit diagram for a sense wire pair of the shaping amplifier module.

spectrometer. These preliminary studies provided us with data for determining optimal values for field wire- and cathode-high voltages, threshold voltages for discriminators, width of ADC gates, and drift time. During the preliminary runs we learned that most of the pickup noise before the preamplifiers was *independent of the high voltage* on the cathodes and field wires, while the magnitude of the signal depended strongly on the voltage. To obtain sufficient primary amplification of the signal over the noise, the cathodes and field wires had to be at least at 1.7 kV. This prompted us to reduce the preamplifiers' (BNL IO354-2) original gain by about a factor of 5 to avoid saturating amplifiers or ADCs at this high voltage. The discriminator threshold was set to about 20 mV to maintain high detection efficiency and to control the noise rates. The gate width of ADCs was set at 50 ns to utilize their dynamic range and allow for variation in pulse arrival time. The drift time in the gas mixture we adopted was about 20 ns/mm at the operating voltage of 1.7 kV.

The primary aim of testing and calibration was to obtain a thorough and detailed understanding of the chamber's gain vs. high voltage and z-position resolution. Measurements of the chamber's performance and position resolution obtained from calibration and testing runs are presented below.

5.1. Gain dependence on cathode voltage

A ^{55}Fe source was used to measure charge amplification and position resolution of the chamber. The 5.9 keV photons emitted by this source generate a highly localized primary ionization charge of about 3.8×10^{-17} C. In Fig. 10 the chamber's signal amplification vs. cathode HV are shown. For the ^{55}Fe source at an operating voltage of

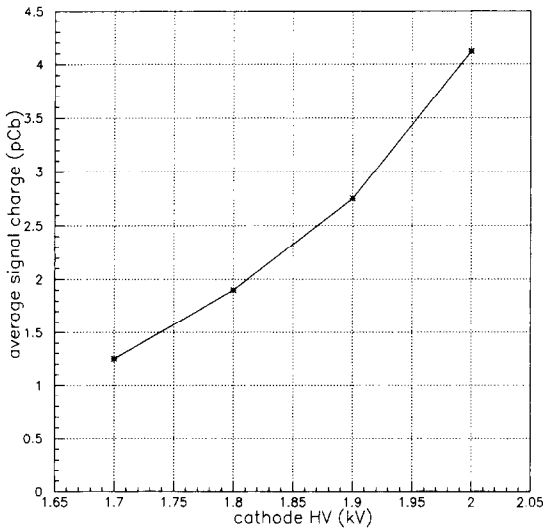

Fig. 10. TCYL signal charge vs. cathode high voltage for the 5.9 keV photons of ^{55}Fe.

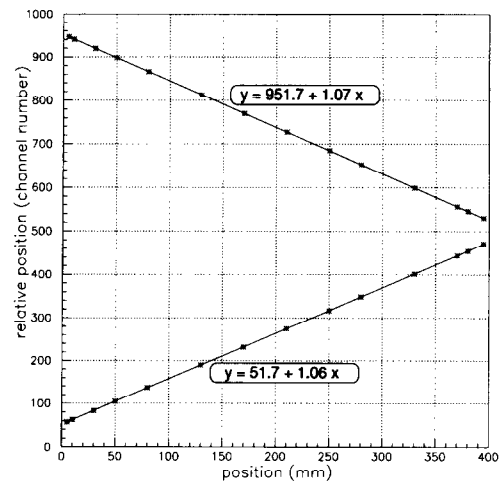

Fig. 11. Longitudinal position calibration via the charge division method with a ^{55}Fe source. Relative position is plotted vs. physical position of the source.

– 1.7 kV the signal charge is 1.3 pC. Thus for a minimum ionizing particle that deposits an average energy of about 2 keV on passage through one layer of the chamber, the signal charge is approximately 0.44 pC for this operating voltage.

5.2. z-position calibration

A collimated ^{55}Fe source with an opening smaller than 1 mm was used for checking the calibration and accuracy of the z (axial) coordinate determination. The source was moved along one of the TCYL cells consisting of a pair of linked sense wires. The position of the source was measured directly and also by detecting the location of its radiation using the charge division method. This method provided a relative position z_r defined as $z_r = Q_1/(Q_1 + Q_2) \times 1000$, where the Q's represent the amounts of charge arriving at the two ends of the wire pair as read by the ADCs.

The results of these measurements are presented in Fig. 11. The data points along the two lines correspond to the hits along the two linked wires. The linearity is excellent. The slope of each line is clearly the conversion factor between channels and millimeters. There is a slight difference (0.8%) between the slopes of the two lines as a result of a small difference between the resistance of the two wires. The average conversion factor for this pair of wires is 1.0643 channels/mm. The effective length of each wire in the pair is 400 mm (875 Ω). The gap of 48.74 channels between the two lines at the 400 mm positions is due to the two 50 Ω resistors between the wires at the downstream end. This gap serves to identify which wire of the pair fired when a hit is close to their connected downstream ends. The charge division method gives outstanding position resolution (~1 mm) along the z-direction in the test with the ^{55}Fe source. This is due to the very localized ionization produced by the 5.9 keV X-rays emitted by the source. The z-resolution for the minimum ionizing particles traversing the chamber, which is a relevant quantity in the performance of the chamber, is discussed in Section 6 below.

The calibration and testing of the chamber using cosmic rays gave us familiarity with its operation and performance. Results of these tests are not presented here since they were superseded by the actual experimental data.

6. Performance

During the years 1993–95 our experiment collected about 10^9 events of various processes. The high statistics was required to provide definitive results for partial wave analyses of meson production in the 1–2 GeV mass range. The task of TCYL during the data acquisition was to impose conditions on the recoil particle but with minimal limitation on the forward-going particles.

TCYL, as a trigger element in the data acquisition, required that interactions with a recoiling proton would have one or more hits in the first, second and third sense wire layer and no more than one hit in the fourth, the outermost layer. The more stringent requirement was imposed only on the fourth layer because its opening provides the largest solid angle for the forward-going particles. Thus, events with forward-going charged tracks that pass through the inner layers of TCYL were not rejected at the trigger level as long as their angle was small enough so that they did not traverse the outermost array.

Similarly, for interactions with a recoiling neutron, TCYL required zero hits in the fourth layer. This placed no restrictions on particles traversing the inner layers. This multiplicity restriction provided us with clean events and reduced the overall trigger rate by a factor of 4.

Off-line, TCYL signals analyzed by TDCs and ADCs provide hit locations along particle trajectories that are used by a pattern recognition program in reconstructing events and in identifying the production vertex. In Fig. 12 we show data from TDCs and ADCs obtained from an experimental run.

Fig. 12a displays the raw data of a TDC taken with a common stop signal derived from a pretrigger. The histogram shows a distribution of drift times for one wire pair. Most of the events fall within 80 ns. Since the distance from the sense wire to both cathodes and field wires is 4 mm, the measured drift time is consistent with an average drift velocity of about 5 cm/μs. This is a common value for electron drift velocity for this gas mixture and high voltage. Fig. 12b shows the TDC value versus distance from the wire as obtained from the reconstructed particle track. Fig. 12c gives the distance error in the azimuthal direction obtained from the TDC drift time. The position resolution of the chamber in azimuthal direction is about 0.4 mm.

Fig. 13a displays the pulse height spectrum of an ADC of one of the sense wire pairs. Fig. 13b gives the z-position of hits along the pair. The forward/backward asymmetry is

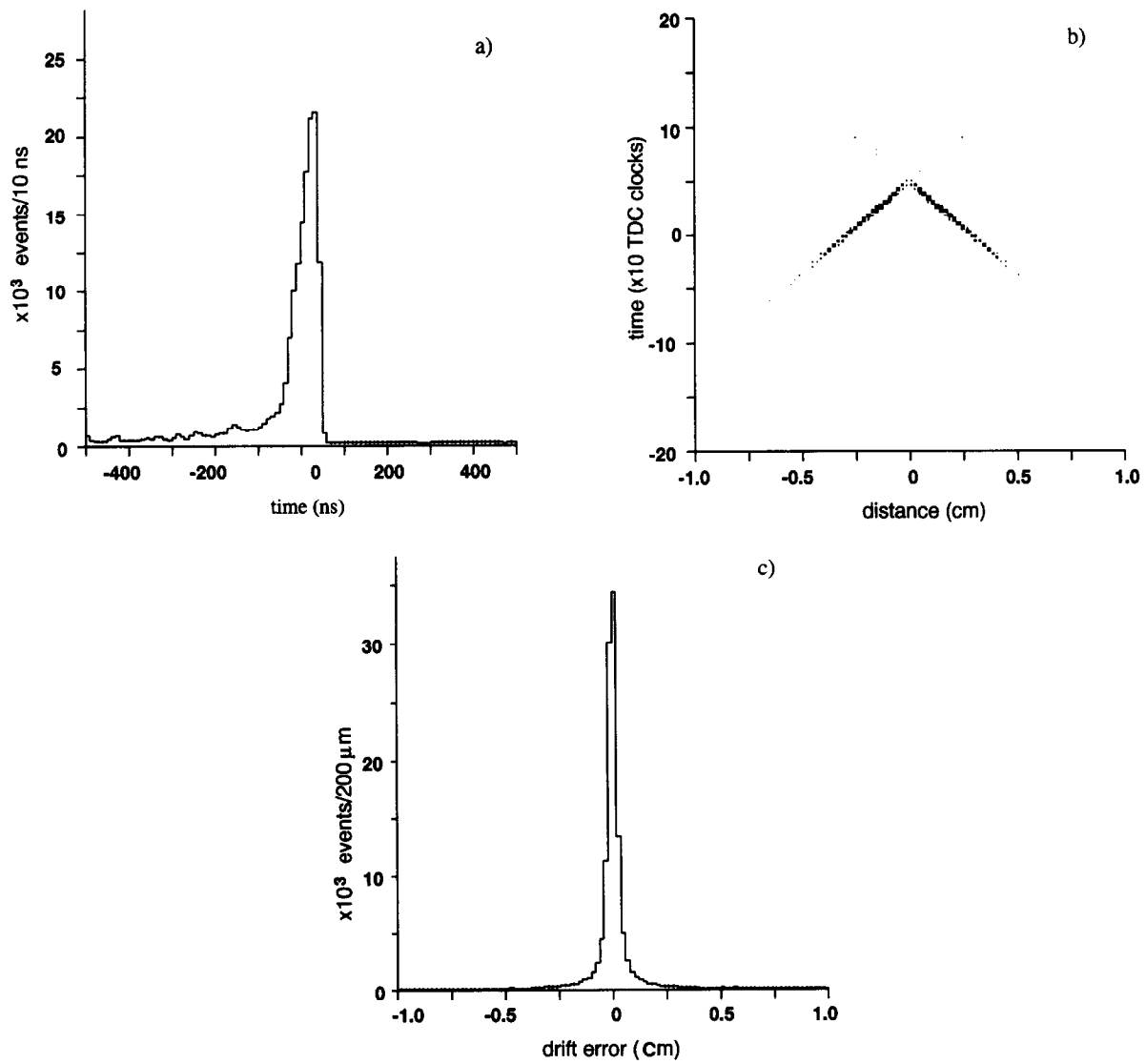

Fig. 12. TCYL performance. The data presented is from the TDCs of the fourth, the outermost, array of sense wires (layer D): (a) TDC distribution (operating with a common stop); (b) TDC drift time vs. track distance from the wire; (c) histogram of the drift distance errors.

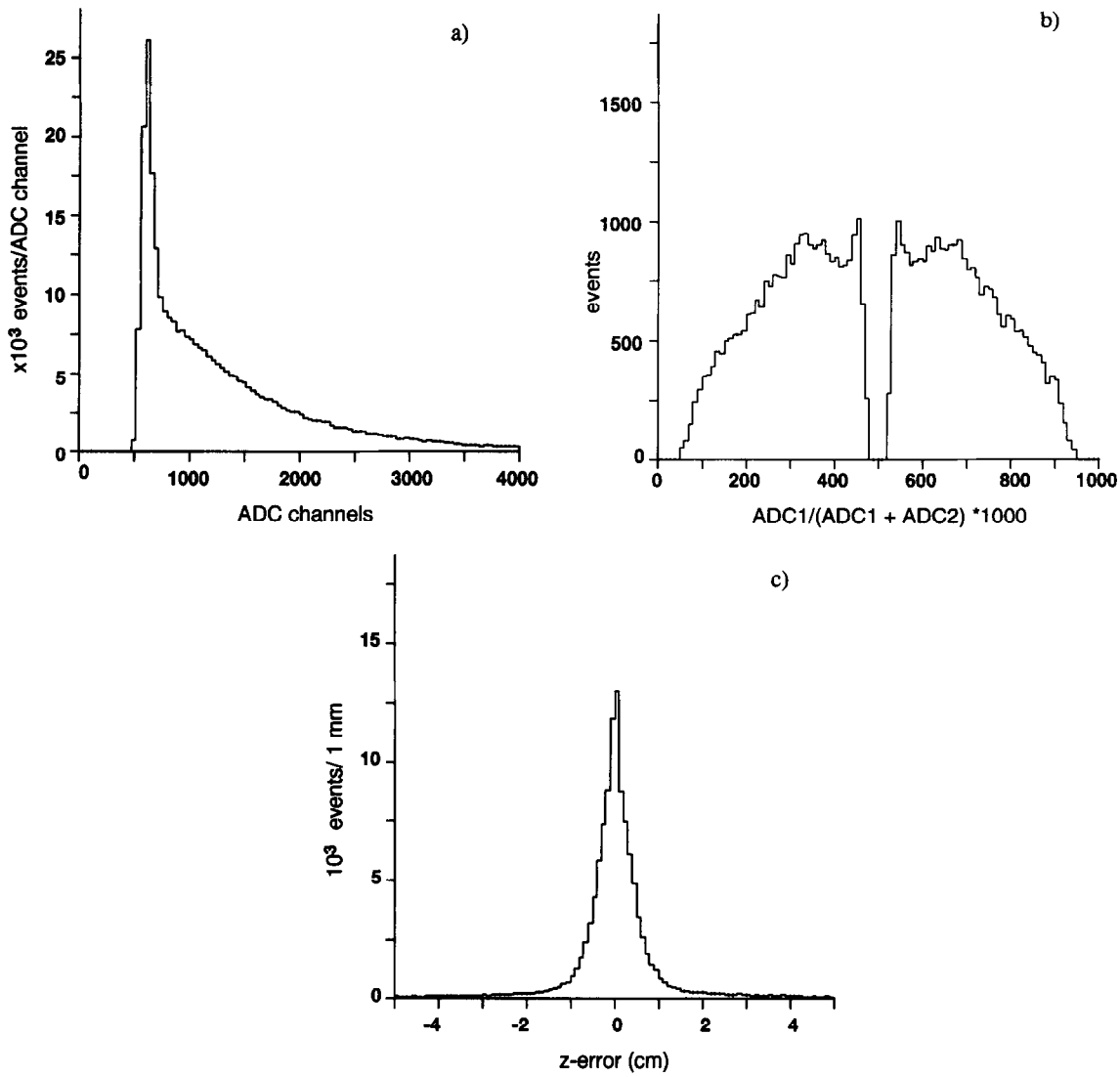

Fig. 13. TCYL performance. Data obtained from the ADCs of the D layer: (a) ADC distribution; (b) relative z-position obtained by charge division; (c) histogram of z-position error.

due to the high momentum of the beam. The empty region in the middle is due to the two 50 Ω resistors that separate the two sense wires to help in identifying which wire in the pair fired. For determining absolute z-position of the hits, the wire end positions were measured by surveying and also by using event reconstruction. Fig. 13c shows the deviation from the track of the z-position obtained from ADCs. The resolution of the chamber in the z-direction is about 7 mm.

An example of a reconstructed event is presented in Fig. 14. Hits in the proportional and drift chambers are indicated and particle trajectories, reconstructed using a pattern recognition program, are shown. The efficiency of each of the cylindrical wire layers was over 97%.

7. Conclusions

A cylindrical drift chamber was constructed and operated successfully during prolonged experimental runs. On-line, during the data taking, it served to reduce the background and identify processes with recoiling protons and neutrons. Off-line, during data processing, it aided in measuring the recoiling proton trajectory, measuring the location of the event vertex and identifying the proton track entering the CsI photon detector.

The special features of the chamber include:

(i) Light weight Rohacell/Kevlar construction.

(ii) Aluminized cathodes laminated onto 1 mm thick walls shared by adjacent drift gaps.

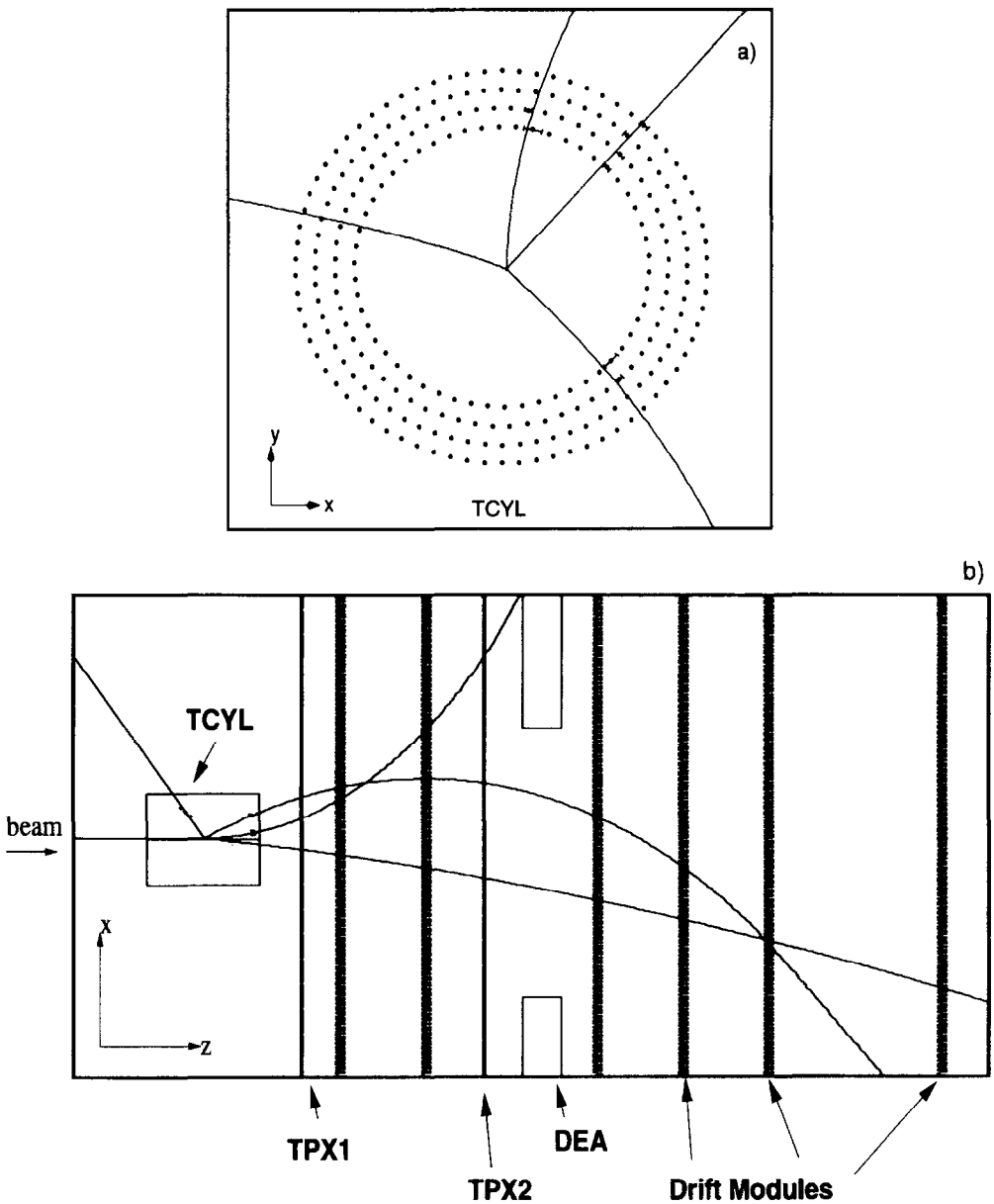

Fig. 14. Event (not to scale) with three forward-going tracks and recoiling proton: (a) x–y view; (b) x–z view.

(iii) Four sensitive independent gaps within overall radial dimension of 63 to 100 mm.

(iv) Pairing of the sense wires by resistive connection on the downstream end to allow charge division signal readout on the upstream end.

(v) Small drift cell size (4 mm) to provide fast response for use in the trigger.

(vi) Over 97% efficiency for each of the four layers.

(vii) Charge division measurement of the axial hit position with a resolution of 7 mm along the 40 cm wire length.

(viii) Ionization drift time measurement of the hit location in the Φ-direction with 0.4 mm accuracy.

Acknowledgments

We wish to acknowledge the many contributions made by the BNL Instrumentation Division. The design of the chamber electronics was made in collaboration with Prof. Veljco Radeka of the BNL Instrumentation Division. The layout of the electronics and its assembly was carried out

by John Hammond of BNL, the development of the preamplifiers and their modification was done under the supervision of Dmitri Stephani of the BNL Instrumentation Division. We also wish to thank other members of Brookhaven National Laboratory for their technical support. In particular, thanks are due to Michael Lenz, Al Roebuck, and Henry Stemm for their guidance and excellent workmanship. We are indebted to the many graduate and undergraduate students from the University of Massachusetts Dartmouth who devoted long hours and care in carrying out this project. In particular, we acknowledge the contributions of Joseph Conery, Richard Coleman, Juewen Zhuang, Syed Faruque, Adam Heath, Ying Ma, Ehsan Monzurul and Jeffrey Schoonover. This work was supported in part by NSF grants PHY-9001389 and PHY-9302063 at the University of Massachusetts Dartmouth, PHY-9120649 at the University of Notre Dame, and PHY-9507412 at Rensselaer Polytechnic Institute; and by DOE grants DE-AC02-76CH00016 at Brookhaven National Laboratory, DE-FG02-91ER40661 at Indiana University, DE-FG02-91ER40623 at the University of Notre Dame, and DE-FG02-87-ER40344 at Northwestern University.

References

[1] Z. Bar-Yam et al., Nucl. Instr. and Meth. A 342 (1994) 398.

[2] B.B. Brabson et al., Nucl. Instr. and Meth. A 332 (1993) 419; R.R. Crittenden et al., Nucl. Instr. and Meth. (submitted).

[3] T. Adams et al., Nucl. Instr. and Meth. A 368 (1996) 617.

[4] N. Shenhav, Nucl. Instr. and Meth. A 324 (1993) 551.

[5] V. Radeka and P. Rehak, IEEE Trans. Nucl. Sci. NS-26 (1978) 46; V. Radeka and P. Rehak, IEEE Trans. Nucl. Sci. NS-25 (1979) 73.

[6] J. Fischer, A. Hrisoho, V. Radeka and P. Rehak, Nucl. Instr. and Meth. A 238 (1985) 249.

[7] R.R. Crittenden et al., Nucl. Instr. and Meth. A 270 (1988) 99.